Supplementary Materials

Isotopic evidence of photoheterotrophy in Palaeoproterozoic Chlorobi

Xiaowen Zhang, Madeline M. Paoletti, Gareth Izon, Gregory P. Fournier and Roger E. Summons

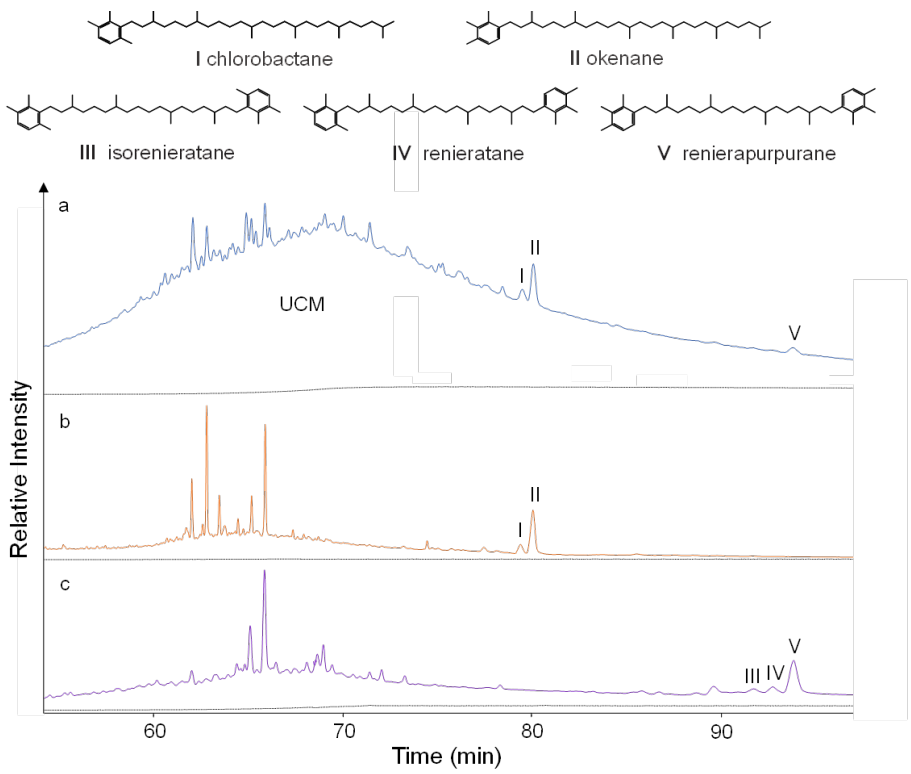

Extended Data Fig.1| Gas chromatographic analysis of sample GR10-130.35m, highlighting the effectiveness of our mordenite cleaning protocol. Here, the full-scan GC-MS total ion chromatogram (TIC) in panel A illustrates the total aromatic fraction obtained via by conventional Si-gel chromatography, while those in the lower panels depict the mordenite-cleaned (i.e., included) monoaromatic (B) and diaromatic (C) fractions. Panel A clearly shows the problematic UCM that has, until now, precluded isotopic analysis of the Barney Creek carotenoids; panels B–C, however, illustrate the effectiveness of our mordenite-based cleaning protocol. Here, and elsewhere, the peaks and structures labelled I–V denote chlorobactane, okenane, isorenieratane, renieratane and renierapurpurane, respectively.

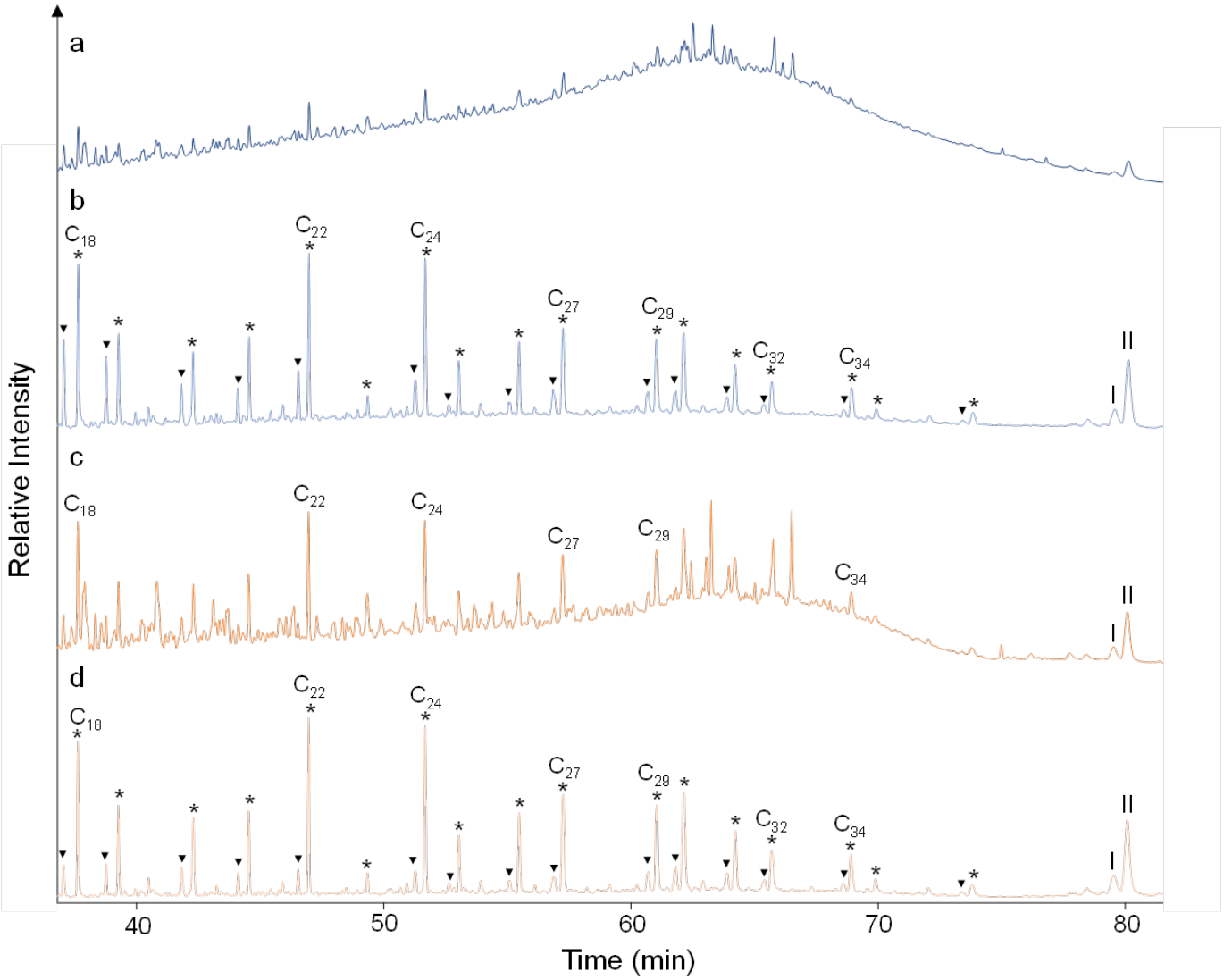

Extended Data Fig.2| Gas chromatographic analysis of the monoaromatic fraction isolated from sample GR10-133.8m. Panels A and B give the respective total ion and secondary ion (m/z = 134) chromatograms of the unprocessed monoaromatic fraction, while panels C and D show their mordenite cleaned equivalents (i.e., the included fraction; methods). Triangles and stars distinguish 2,3,6- and 2,3,4-trimethyl aryl isoprenoids, while chlorobactane and okenane are identified by I and II, respectively.

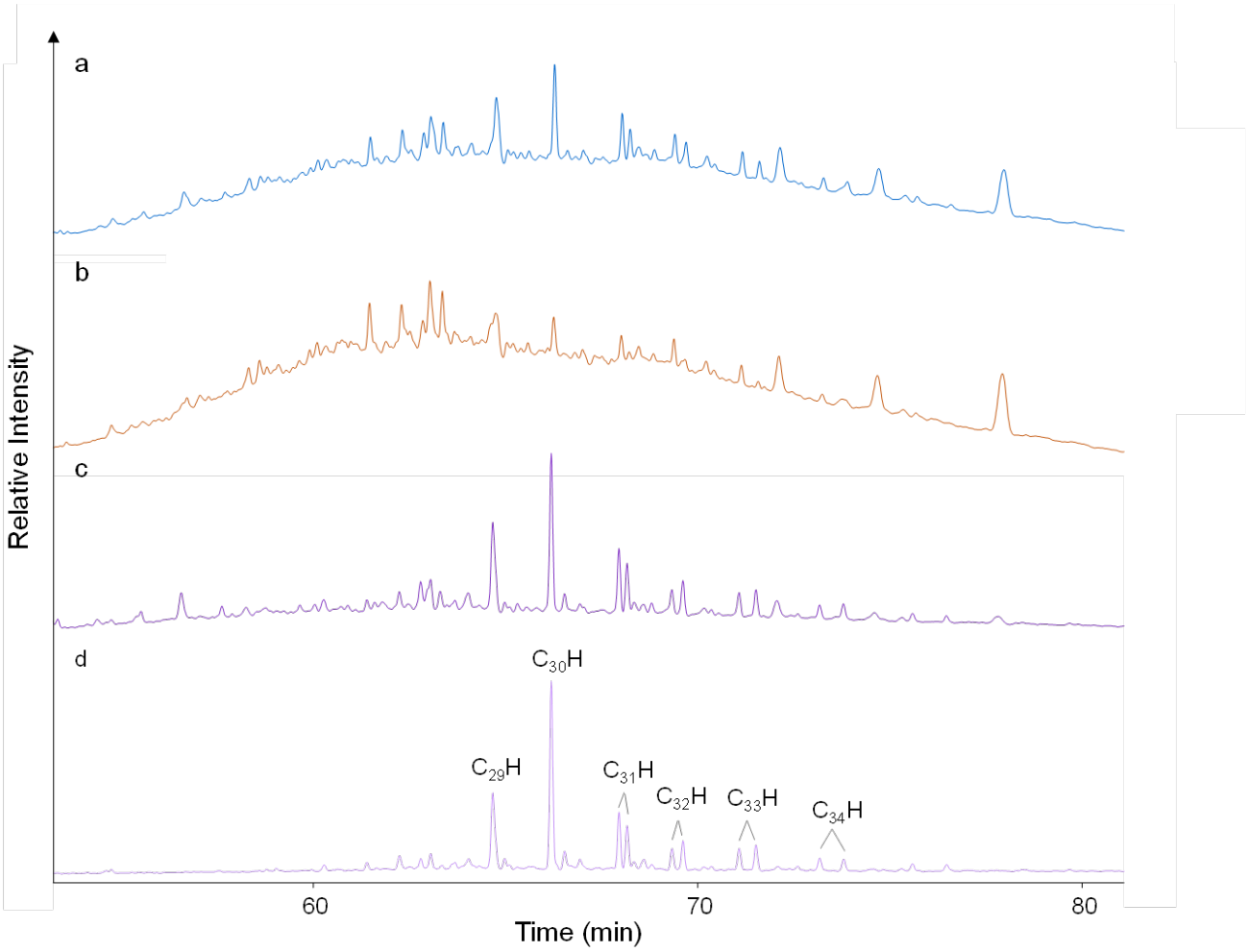

Extended Data Fig.3| Gas chromatographic analysis of sample GR10:130.35m showing the influence of our 13X-cleaning protocol. Panel A shows the total ion chromatogram (TIC) of the conventionally obtained saturate fraction, while panels B and C give the 13X-excluded and -included fractions, respectively. Comparison of these panels shows that most of the problematic matrix is retained in the free lipid fraction (i.e., the 13X-excluded fraction), resulting in a significantly reduced background and well resolved hopane peaks after HF dissolution. Monitoring m/z 191, panel D gives a selected ion chromatogram where various hopanes are identified. Here, $C_{29}H$ and $C_{30}H$ denotes 17α,21β hopanes while $C_{31\text{-}34}H$ denotes 17α,21β homohopanes, with S (left) and R (right) configurations at C-22 (Supplementary Table 2).

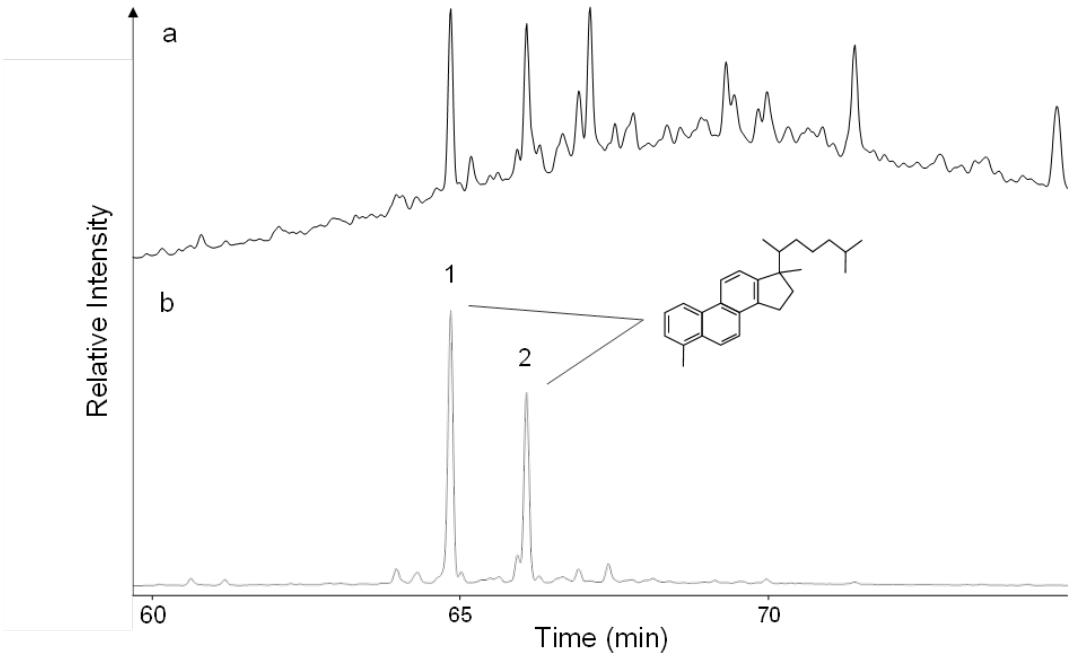

Extended Data Fig.4| Gas chromatographic analysis of the polyaromatic fraction isolated from sample GR10-117.8m. Panel A and B give total ion and selected ion (m/z = 245) chromatograms, respectively. The identified peaks in panel B are 4-methyl triaromatic steroids.

Supplementary Table 1. Total organic carbon (TOC) and carbonate abundances (Wt. %) of the examined Barney Creek samples. n.d. is not determined.

Sample Identifier	GR10-85.7m	GR10-103.5m	GR10-117.8m	GR10-124.7m	GR10-130.35m	GR10-133.8m	GR10-141.9m	GR10-157.3m	GR10-167.8m	GR10-182.8m
TOC	2.0	0.5	0.2	0.4	0.6	1.9	5.0	1.0	1.2	3.2
Carbonate	3.1	n.d	n.d	6.7	n.d	5.4	3.3	6.0	5.2	2.7

Supplementary Table 2. Carbon isotope signatures ($\delta^{13}C$; ‰) of bulk and interior biomarker constituents of the Barney Creek Formation. Here, the tabulated n-alkane $\delta^{13}C$ value represents the average value calculated from those determined from the C_{14}–C_{30} n-alkanes (Supplementary Table 3). Hopanes are identified within the representative gas chromatograms given in Extended Data Fig.3. Standard deviation of duplicates less than 0.4 ‰ was replaced by the maximum isotopic difference (0.4‰) of a single compound in A5 n-alkane standards (Methods).

	Sample Identifier	GR10-85.7m	GR10-103.5m	GR10-117.8m	GR10-124.7m	GR10-130.35m	GR10-133.8m	GR10-141.9m	GR10-157.3m	GR10-167.8m	GR10-182.8m
Analysed compound ($\delta^{13}C$; ‰)	Carbonate	-1.0			-0.4		-0.4	-0.6	-0.3	-0.5	-0.6
	TOC	-31.7	-32.1	-31.5	-31.2	-31.1	-31.1	-30.4	-31.1	-31.3	-30.5
	n-Alkanes	-29.2 ±0.8		-30.1 ±0.6			-29.4 ±0.6	-28.8 ±0.8	-28.8 ±0.7	-29.6 ±0.7	-28.3 ±0.9
	Chlorobactane		-33.8 ±0.4	-35.6 ±0.9		-34.3 ±0.4					
	Okenane		-35.6 ±0.4	-36.5 ±0.4		-35.8 ±0.4	-35.9 ±1.0	-35.4 ±1.1	-37.6 ±1.2		
	Isorenieratane		-35.0 ±1.2[a]			-33.9 ±1.8[a]					
	Renieratane					-38.8 ±0.4[a]					
	Renierapurpurane		-37.9 ±0.5[a]	-37.5 ±0.4	-37.2 ±0.7	-37.5 ±0.6					
	2,3,4-Aryl isoprenoids	-33.5 ±0.4					-35.5 ±0.4				-34.0 ±0.4
	β-carotane		-36.3 ±0.4	-37.7 ±0.5		-37.9 ±0.4					
	γ-carotane		-35.6 ±0.4[a]	-36.5 ±0.4		-36.6 ±0.4[a]					
	Pristane	-32.2 ±0.9*		-31.4 ±0.4*			-32.4 ±0.4*	-31.3 ±1.0*		-32.4 ±0.8*	
	Phytane	-32.6 ±0.4		-32.5 ±0.9			-33.5 ±0.4	-32.5 ±1.1		-32.6 ±0.4	
	i-21	-32.3 ±0.6		-32.9 ±0.8			-33.6 ±0.8	-31.2 ±1.8		-31.0 ±1.6[a]	
	i-23	-32.3 ±0.8		-32.9 ±0.4			-31.9 ±0.4	-31.4 ±0.4		-31.6 ±0.4[a]	
	C_{30} αβ hopane		-30.9 ±0.4*	-29.1 ±0.4*		-29.9 ±0.6*	-25.8 ±0.9*	-27.5 ±0.6*	-29.2 ±0.6*	-27.6 ±0.5*	
	C_{31} αβ-22S hopane		-32.6 ±0.4			-32.0 ±1.0		-28.2 ±0.6			
	C_{31} αβ-22R hopane		-29.5 ±1.3			-29.8 ±0.4		-27.7 ±0.4			
	C_{32} αβ-22S hopane		-33.9*			-33.3 ±0.4*					
	C_{32} αβ-22R hopane		-31.6*			-32.0 ±0.7*					
	C_{33} αβ-22S hopane		-32.8[a]			-34.1 ±0.8[a]					
	C_{33} αβ-22R hopane		-30.8[a]			-32.7 ±0.7[a]					

[a] low intensity. *minor coelution with similar carbon isotope values.

Supplementary Table 3. The carbon isotope composition of C_{14}–C_{30} n-alkanes isolated from the Barney Creek Formation. The quoted uncertainty, given in parentheses, is the standard deviation of duplicate measurements larger than 0.4‰. n.d. is not determined. Sample 103.5m, 124.7m, and 130.35 have little n-alkanes thus are not measured.

Sample Identifier	$\delta^{13}C$ (‰), carbon number																
	14	15	16	17	18	19	20	21	22	23	24	25	26	27	28	29	30
GR10-85.7m	-29.7	-29.8	-29.7	-29.8	-29.7	-29.5	-29.6	-29.9	-30.0	-29.8	-29.5	-28.6	-28.6	-27.9	-28.2	-28.0	-28.3
GR10-117.8m	-31.2 (0.6)	-30.3	-30.5	-30.9	-30.6	-30.7	-30.1	-29.8	-29.8	-29.9	-29.8	-29.3	-29.3 (0.5)	-29.8	-29.5	-30.2	-29.7
GR10-133.8m	-29.8	-29.8	-30.1	-30.4	-30.2	-30.0	-29.7	-29.6	-29.7	-29.2	-28.9	-29.3	-28.5	-28.9	-28.5	-28.6	-28.6
GR10-141.9m	-29.7	-29.8	-29.8	-29.8	-29.6	-29.5	-29.3	-29.1	-28.7	-28.2	-28.3	-28.1	-27.7	-28.1	-28.2	-27.6	-28.2
GR10-157.3m	-29.3	-29.4	-29.6	-29.9	-29.6	-29.5	-29.2	-28.8	-28.8	-28.4	-28.1	-28.4	-28.0	-28.6	-28.2	-28.2	-27.5
GR10-167.8m	-30.1	-29.9	-30.4	-30.3	-30.2	-30.2	-30.2	-30.1	-29.6	-29.8	-28.8	-28.6	-28.9	-29.2	-28.4	n.d.	n.d.
GR10-182.8m	-29.3	-29.4	-29.0	-29.4	-29.3	-29.2	-29.1	-28.7	-28.5	-28.0	-27.6	-27.6	-27.2	-27.3	-27.3	-27.2	-27.5

Supplementary Table 4: The carbon isotope composition of aromatic carotenoids isolated from the exterior layers of selected samples to check the potential impact of contamination on isotope results. Quoted uncertainties are standard deviation of duplicate measurements.

Sample Identifier	$\delta^{13}C$ (‰)				
	Chlorobactane	Okenane	Isorenieratane	Renieratane	Renierapurpurane
GR10-89.2m		-34.3 ±0.6			-36.8 ±0.4
GR10-130.35m	-35.0 ±0.7	-36.1 ±0.4	-35.5 ±1.9	-38.5 ±0.4	-38.3 ±0.4
GR10-133.8m		-34.6 ±0.4			

Supplementary Table 5: Carbon isotope data from the methodological tests. Here, the $\delta^{13}C$ values of unprocessed materials (Original) are compared with those measured from the bound (Included) and free (Excluded) fractions after purification with a 13X molecular sieve and mordenite (methods). Standard deviations of duplicates are all within the maximum isotopic difference (0.4‰) of duplicated A5 standards. n.d. is not determined.

Analyte (purification technique)	$\delta^{13}C$ (‰)		
	Original	Included	Excluded
pristane (13X)	-31.8	-31.2	-31.5
phytane (13X)	-32.7	-32.8	-32.1
2,3,6-C_{14} aryl isoprenoid (mordenite)	-34.2	n.d.	-34.1

Supplementary Table 6: Carbon isotope values of aromatic carotenoids and 2,3,6-aryl isoprenoids compiled from the literature. Quoted uncertainties, if given, follow their source. Data from the Miocene and younger are derived from the biological precursor to isorenieratane, isorenieratene

Analyte, Location	Epoch	Age (Ma)	$\delta^{13}C$ (‰)			Source
			Isorenieratane	Chlorobactane	2,3,6-aryl isoprenoid	
Boas Oil Shale	Late Ordovician	443.8–458.4			-18.9	(Koopmans et al., 1996)
Ram oils, Michigan Basin	Silurian	419.2–443.8			-24.7 to -21.6	(Summons and Powell, 1986)
Duvernay Fm.	Late Devonian	372.2–382.2	-13.2 to -5.2		-17.7 to -14.2	(Hartgers et al., 1994)
Holy Cross Mountains	Late Devonian	358.9–382.7	-16.5 to -13.2			(Joachimski et al., 2001)
Kupferschiefer, Lower Rhine Basin	Late Permian	255.7–258.9	-16.4 to -13.4		-20.4 to -15.6	(Grice et al., 1996)
St Audrie's Bay	Late Triassic	201.3–208.5	-16			(Jaraula et al., 2013)
Frick Swiss Jura sediments	Early Jurassic	190.8–201.3			-22.6 to -15.4	(Schwab and Spangenberg, 2007)
Allgäu Fm.	Early Jurassic	174.1–182.7	-19.0			(Sinninghe Damsté et al., 1995a)
Paris Basin	Early Jurassic	174.1–182.7	-14.8 to -9.8			(van Breugel et al., 2006)
Kimmeridge Clay Fm.	Late Jurassic	152.1–157.3	-16.6			(Sinninghe Damsté et al., 1995b)
Calcaires en plaquettes Fm.	Late Jurassic	152.1–157.3	-19			(Koopmans et al., 1996)
Maculungo Fm., Kwanza Basin	Early Cretaceous	129.4–145.0	-14.4			(Pedentchouk et al., 2004)
Demerara Rise	Late Cretaceous	90–100.5	-17.6 to 16.5			(Sinninghe Damsté and Köster, 1998)
Cape Verde Basin (DSDP 367)	Late Cretaceous	90–100.5	-15.9 to -10.7			(Sinninghe Damsté and Köster, 1998; Sinninghe Damsté et al., 2008)
Tarfaya coastal basin	Late Cretaceous	90–100.5	-13.2 to -11.6			(Sinninghe Damsté and Köster, 1998)
Lomonosov Ridge	Early Eocene	50–56	-26.3 to -21.4			(Schoon et al., 2011)
Xingouzui Fm., Jianghan Basin	Early Eocene	47.8–56	-17.3 to -17.0			(Grice et al., 1998)
Qianjiang Fm., Jianghan Basin	Late Eocene	33.9–28	-16.5 to -16.1	-16.6		(Grice et al., 1998)
Gessoso-solfifera Fm.	Late Miocene	5.3–7.2	-16.4 to -12.4			(Koopmans et al., 1996; Putschew et al., 1998)
Black Sea	Holocene	0.006	-17.4 to -14.8*			(Sinninghe Damsté et al., 1993)

*Isorenieretene

S3. Appendix

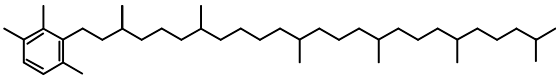

I chlorobactane

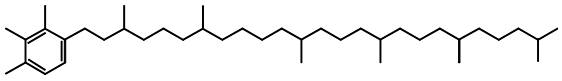

II okenane

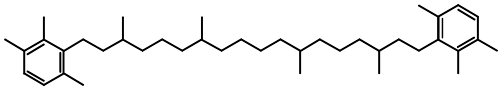

III isorenieratane

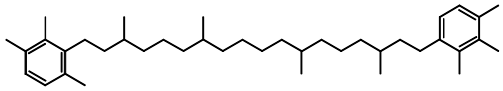

IV renieratane

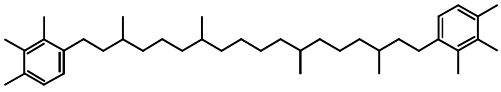

V renierapurpurane

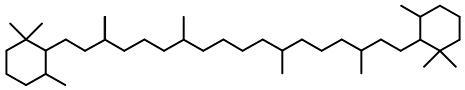

VI β-carotane

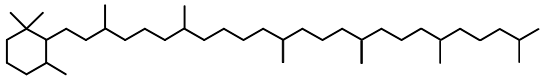

VII γ-carotane

S4. Supplementary References

Grice, K., Schaeffer, P., Schwark, L., Maxwell, J.R., 1996. Molecular indicators of palaeoenvironmental conditions in an immature Permian shale (Kupferschiefer, Lower Rhine Basin, north-west Germany) from free and S-bound lipids. Organic Geochemistry 25, 131-147.

Grice, K., Schouten, S., Peters, K.E., Damsté, J.S.S., 1998. Molecular isotopic characterisation of hydrocarbon biomarkers in Palaeocene–Eocene evaporitic, lacustrine source rocks from the Jianghan Basin, China. Organic Geochemistry 29, 1745-1764.

Hartgers, W.A., Damsté, J.S.S., Requejo, A., Allan, J., Hayes, J.M., Ling, Y., Xie, T.-M., Primack, J., de Leeuw, J.W., 1994. A molecular and carbon isotopic study towards the origin and diagenetic fate of diaromatic carotenoids. Organic Geochemistry 22, 703-725.

Jaraula, C.M., Grice, K., Twitchett, R.J., Böttcher, M.E., LeMetayer, P., Dastidar, A.G., Opazo, L.F., 2013. Elevated p CO2 leading to Late Triassic extinction, persistent photic zone euxinia, and rising sea levels. Geology 41, 955-958.

Joachimski, M.M., Ostertag-Henning, C., Pancost, R.D., Strauss, H., Freeman, K.H., Littke, R., Damste, J.S.S., Racki, G., 2001. Water column anoxia, enhanced productivity and concomitant changes in δ13C and δ34S across the Frasnian–Famennian boundary (Kowala—Holy Cross Mountains/Poland). Chemical Geology 175, 109-131.

Koopmans, M.P., Köster, J., Van Kaam-Peters, H.M., Kenig, F., Schouten, S., Hartgers, W.A., de Leeuw, J.W., Damsté, J.S.S., 1996. Diagenetic and catagenetic products of isorenieratene: Molecular indicators for photic zone anoxia. Geochimica et Cosmochimica Acta 60, 4467-4496.

Pedentchouk, N., Freeman, K.H., Harris, N.B., Clifford, D.J., Grice, K., 2004. Sources of alkylbenzenes in Lower Cretaceous lacustrine source rocks, West African rift basins. Organic Geochemistry 35, 33-45.

Putschew, A., Schaeffer, P., Schaeffer-Reiss, C., Maxwell, J.R., 1998. Carbon isotope characteristics of the diaromatic carotenoid, isorenieratene (intact and sulfide-bound) and a novel isomer in sediments. Organic geochemistry 29, 1849-1856.

Schoon, P.L., Sluijs, A., Sinninghe Damsté, J.S., Schouten, S., 2011. Stable carbon isotope patterns of marine biomarker lipids in the Arctic Ocean during Eocene Thermal Maximum 2. Paleoceanography 26.

Schwab, V.F., Spangenberg, J.E., 2007. Molecular and isotopic characterization of biomarkers in the Frick Swiss Jura sediments: A palaeoenvironmental reconstruction on the northern Tethys margin. Organic Geochemistry 38, 419-439.

Sinninghe Damsté, J.S., Kenig, F., Koopmans, M.P., Köster, J., Schouten, S., Hayes, J., de Leeuw, J.W., 1995a. Evidence for gammacerane as an indicator of water column stratification. Geochimica et Cosmochimica Acta 59, 1895-1900.

Sinninghe Damsté, J.S., Köster, J., 1998. A euxinic southern North Atlantic Ocean during the Cenomanian/Turonian oceanic anoxic event. Earth and Planetary Science Letters 158, 165-173.

Sinninghe Damsté, J.S., Koster, J., Baas, M., Koopmans, M.P., van Kaam-Peters, H.M., Geenevasen, J.A., Kruk, C., 1995b. Cyclisation and aromatisation of carotenoids during sediment diagenesis. Journal of the Chemical Society, Chemical Communications, 187-188.

Sinninghe Damsté, J.S., Kuypers, M.M., Pancost, R.D., Schouten, S., 2008. The carbon isotopic response of algae,(cyano) bacteria, archaea and higher plants to the late Cenomanian perturbation of the global carbon cycle: Insights from biomarkers in black shales from the Cape Verde Basin (DSDP Site 367). Organic Geochemistry 39, 1703-1718.

Sinninghe Damsté, J.S., Wakeham, S.G., Kohnen, M.E., Hayes, J., de Leeuw, J.W., 1993. A 6,000–year sedimentary molecular record of chemocline excursions in the Black Sea. Nature 362, 827-829.

Summons, R.E., Powell, T.G., 1986. Chlorobiaceae in Palaeozoic seas revealed by biological markers, isotopes and geology. Nature 319, 763-765.

van Breugel, Y., Baas, M., Schouten, S., Mattioli, E., Sinninghe Damsté, J.S., 2006. Isorenieratane record in black shales from the Paris Basin, France: Constraints on recycling of respired CO2 as a mechanism for negative carbon isotope shifts during the Toarcian oceanic anoxic event. Paleoceanography 21.